Exciton localization and structural disorder of $GaAs_{1-x}Bi_x$/GaAs quantum wells grown by molecular beam epitaxy on (311)B GaAs substrates

G.A. Prando[a], V. O. Gordo[a], J. Puustinen[b], J. Hilska[b], H. M. Alghamdi[c], G. Som[d], M. Gunes[d], M. Akyol[d], S. Souto[e], A. D. Rodrigues[a], H. V. A. Galeti[f], M. Henini[c], Y. Galvão Gobato[a], M. Guina[b]

[a] *Departamento de Física, Universidade Federal de São Carlos, 13565-905, São Carlos, SP, Brazil*

[b] *Optoelectronics Research Centre, Tampere University of Technology, P.O. Box 692, FI-33101, Tampere, Finland*

[c] *School of Physics and Astronomy, University of Nottingham, Nottingham NG7 2RD, UK*

[d] *Department of Materials Engineering, Engineering and Natural Sciences Faculty, Adana Science and Technology University, 01250 Adana, Turkey*

[e] *Departamento de Ciências Básicas, Faculdade de Zootecnia e Engenharia de Alimentos, Universidade de São Paulo, 13635-900, Pirassununga, SP, Brazil*

[f] *Departamento de Engenharia Elétrica, Universidade Federal de São Carlos, 13565-905, São Carlos, SP, Brazil*

Keywords: dilute bismides, exciton localization, structural disorder, photoluminescence

Abstract: In this work, we have investigated the structural and optical properties of $GaAs_{(1-x)}Bi_x$/GaAs single quantum wells (QW) grown by molecular beam epitaxy (MBE) on GaAs (311)B substrates using x-ray diffraction (XRD), atomic force microscopy (AFM), Fourier-transform Raman (FT-Raman) and photoluminescence (PL) spectroscopy techniques. The FT-Raman results revealed a decrease of the relative intensity ratio of transverse (TO) and longitudinal (LO) optical modes with the increase of Bi concentration which indicates reduction of the structural disorder with increasing Bi incorporation. In addition, the PL results show an enhancement of the optical efficiency of the structures as the Bi concentration is increased due to important effects of exciton localization related to Bi defects, non-radiative centers and alloy disorder. These results provide evidence that Bi is incorporated effectively in the QW region. Finally, the temperature dependence of PL spectra has evidenced two distinct types of defects related to the Bi incorporation, namely Bi clusters and pairs, and alloy disorder and potential fluctuation.

Introduction

III-V bismide alloys, such as $GaAs_{(1-x)}Bi_x$, are promising materials for optoelectronics applications in the mid-infrared range[1,2]. It is well known that the incorporation of a small amount of Bi in GaAs results in important changes of its physical properties such as significant band gap energy reduction (about 88 meV / Bi % [1,3-5]) and increase of the spin-orbit band splitting. The latter can reduce the non-radiative Auger recombination[6,7] and enhance the Rashba spin-orbit interaction which are important for spintronic[8] and optoelectronic device applications. However, Bi incorporation can also have detrimental effects such as structural disorder and carrier localization which could limit its use for device applications[9-11]. In fact, when the isovalent impurity Bi is incorporated by replacing As in GaAs, the energy levels of Bi strongly interact with valence band states, leading to changes in the electronic band structure[5]. These changes are usually explained by the anticrossing interaction model for valence band[5,9]. However, in order to incorporate bismuth atoms into GaAs host lattice, the alloy must be grown at much lower temperatures (below 400°C) as compared to GaAs optimal growth conditions, and near-stoichiometric III/V flux ratios[12,13]. These growth conditions can introduce important structural defects and disorder, and thus degrade the material quality[14,15]. Due to the large difference between the atomic volume of Bi (21.3 cm^3/g atoms) and As (13.1 cm^3/g atoms), the crystalline structure presents inhomogeneities such as point and extended defects, formation of clusters and pairs of Bi, resulting in a highly perturbed alloy with strong carrier localization effects[10,11,16-19].

Although most investigations of $GaAs_{(1-x)}Bi_x$ films and heterostructures were performed using the conventional GaAs (100) substrate, there are few studies exploring the growth on high index planes which can influence considerably the Bi incorporation and consequently their electrical and optical properties[20-23]. For example, the highest Bi incorporation into (100) GaAs host matrix for $GaAs_{1-x}Bi_x$ films has been empirically reported to be x=0.22 [24]. However, it has been shown that an enhancement of Bi incorporation in GaAsBi thin films can be obtained by using (311)B orientation[20]. In addition, it is worth noting that the structural and optical properties of $GaAs_{(1-x)}Bi_x$ quantum wells (QW) grown on (311)B GaAs substrates have not been investigated yet.

In this paper, we report on the structural, morphological and optical properties of $GaAs_{(1-x)}Bi_x$/GaAs single QW grown by MBE on (311)B GaAs substrates at 320°C with different nominal Bi contents (x= 1 %, 2 %, 3 %). We have performed XRD, AFM, FT-Raman and PL measurements as function of temperature and excitation power (P_{EXC}). The XRD results

evidence that our samples have good crystalline quality. In addition, AFM data show low surface roughness values for all samples. The FT-Raman spectra indicate reduction of the structural disorder with increasing Bi incorporation. Furthermore, PL measurements have demonstrated important effects associated to exciton localization. Finally, our work presents a first detailed investigation of the influence of Bi content on the structural, morphological and optical properties of Bi-containing III-V semiconductor QWs grown on GaAs (311)B substrates.

Experimental details

Our heterostructures consist of 10 nm $GaAs_{1-x}Bi_x$ /GaAs single QWs grown by solid-source MBE on semi-insulating undoped GaAs (311)B oriented substrates, with nominal Bi concentrations x = 1%, 2% and 3%. The growth of the samples started with a 370 nm thick GaAs buffer layer. The first 300 nm was grown at 580 °C and high As overpressure, after which the growth temperature was decreased to 320°C during the growth of an additional 70 nm of GaAs, to enhance the incorporation of Bi in the QW. This was followed by a 10 nm thick GaAsBi QW layer which was capped by a 50 nm GaAs layer grown at the same temperature (see Fig.1). The growth rate was 0.4 µm/h for all layers. For efficient Bi incorporation, the atomic Ga/As flux ratio was adjusted close to the stoichiometric value before the growth of the of the QW.

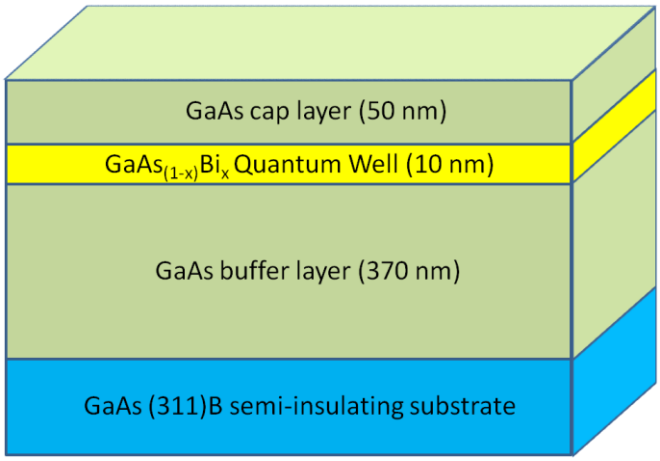

Figure 1. Typical structure of $GaAs_{(1-x)}Bi_x$/GaAs QW grown on (311)B GaAs substrates

The FT-Raman measurements were performed at room temperature in the backscattering geometry using Vertex 70 Bruker equipped with RAM II: FT-Raman module. The samples were optically excited by a 1064 nm line of a solid state laser with an excitation power of 85 mW and measured with a spectral resolution of 1 cm^{-1} and 200 scan accumulations. The PL studies were obtained by using a 0.5 m Spex-Jobin Yvon monochromator with nitrogen-cooled Ge detector and a 532 nm linearly-polarized line CW diode laser for optical excitation. The PL spectra were measured as function of temperature (20 - 300 K) and laser excitation power. High-resolution XRD rocking curves were obtained using a Phillips X'Pert Pro diffractometer for the (311) reflection. AFM images were taken with Veeco Dimension 3100 in the tapping mode.

Results and discussion

XRD rocking curves from each GaAsBi sample are shown in Fig. 2. All diffractograms exhibit distinct thickness fringes around the (311) diffraction maximum, which is an indication of good crystalline quality for the samples[25,26]. Fig. 3 illustrates a typical 5x5 μm^2 AFM image of the (311)B sample with the highest nominal Bi content (3%), which acts as representative of the surface features observed for all GaAsBi samples grown on (311)B GaAs substrates. Despite these observed features, which could be attributed to the not fully optimized growth process on the (311)B substrates, the root mean square surface roughness has a good and acceptable value of 6.00 nm.

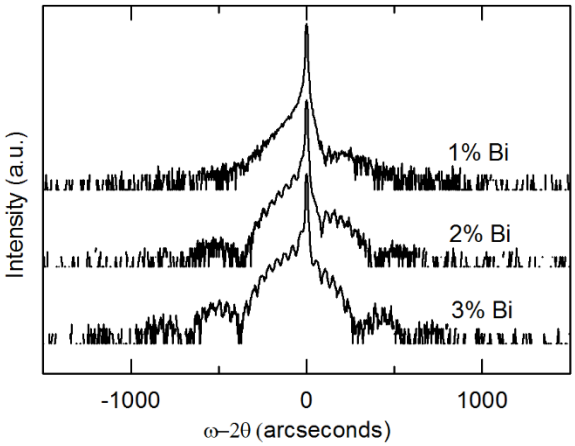

Figure 2. XRD rocking curves of all samples. The measurements are offset in intensity and centered at the (311) reflection maximum.

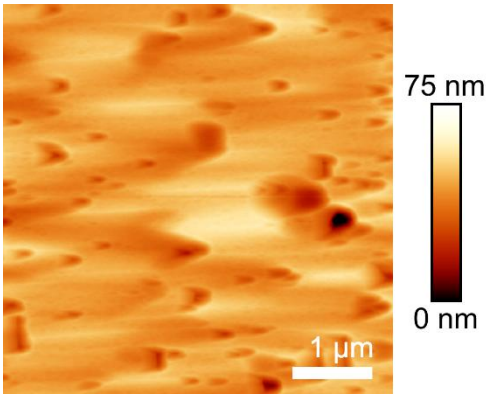

Figure 3. A 5x5 µm^2 AFM image taken from the 3% Bi sample surface.

We have also performed FT-Raman measurements in the range of 30 to 300 cm^{-1} at room temperature using a 1064 nm laser. At this experimental condition, we have important laser penetration in the QW region and the enhancement of Raman signal intensity due to the fact that the incident photon energy is close to the resonant excitation condition. All samples were mounted in a sample holder which allowed crystal rotation with respect to linear polarization of the laser. As expected, we observed a significant dependence of Raman modes for different orientations (not shown here) in agreement with previous investigations[22,27]. Fig. 5 shows typical Raman spectra for different Bi% measured at a specific crystal orientation as will be explained below. In general, we have observed two most prominent peaks attributed to GaAs optical phonon modes in the region 260 to 300 cm^{-1}. The peak at 290 cm^{-1} is attributed to GaAs longitudinal optical phonons (LO_{GaAs}) while the peak detected at 268 cm^{-1} is assigned to GaAs transverse optical phonons (TO_{GaAs}). A strong dependence of Raman peaks with sample orientation was observed, particularly for the relative intensity of LO (I_{LO}) and TO (I_{TO}) GaAs modes. All FT-Raman spectra shown in Fig.4 were obtained at the same crystal orientation which corresponds to the configuration of maximum value of I_{TO}/I_{LO} ratio. In addition, changes in the relative intensities of TO and LO modes with increasing Bi% were detected, which can be related to the disorder introduced by Bi incorporation. To analyze in more detail the disorder effects in these samples, we have studied the Bi dependence on the intensity ratio of I_{TO}/I_{LO} and full width at half maximum (FWHM) (Table 1). Interestingly, a decrease of the relative intensity I_{TO}/I_{LO} with increasing Bi% was observed which indicates some change in the structural disorder due to the incorporation of Bi[23]. This result is consistent with PL data as will be discussed below. Furthermore, a small shift of TO mode was detected with increasing Bi concentration. However, no significant change in the FWHM of LO and TO modes with increasing Bi% content was observed.

In addition, the Disorder-Activated Transverse Acoustic (DATA) around 80 cm^{-1} and Disorder-Activated Longitudinal Acoustic (DALA) around 160 cm^{-1} were measured[22]. They have lower Raman intensities in comparison with LO_{GaAs} and TO_{GaAs} modes and different nature. The observation of DATA and DALA modes also evidences important effects of disorder due to the growth of $GaAs_{(1-x)}Bi_x$/GaAs QW at lower temperatures.

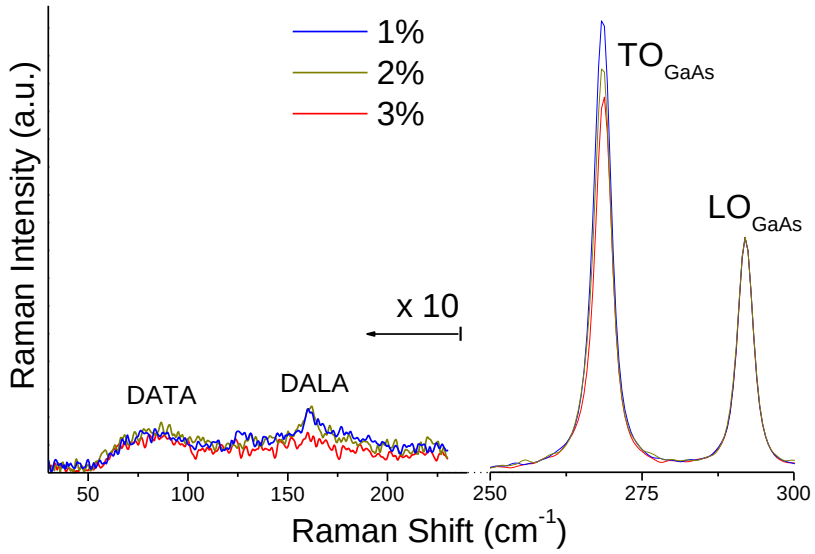

Figure 4. FT-Raman spectra at room temperature for samples with 1%,2% and 3% Bi excited with a 1064 nm laser.

Table 1- Wavenumber, FWHM and relative intensities of TO and LO Raman modes for different concentrations of Bi.

Sample	TO_{GaAs} (cm^{-1})	LO_{GaAs} (cm^{-1})	I_{TO}/I_{LO}	FWHM – TO_{GaAs} (cm^{-1})	FWHM – LO_{GaAs} (cm^{-1})
1% Bi	268,3	292,4	1,92	3.34	3.12
2% Bi	268,3	292,4	1,72	3.44	3.12
3% Bi	268,8	292,4	1,59	3.32	3.14

Fig.5 shows the normalized PL spectra of the QW samples at low temperature (20K). The peaks are related to exciton ground state recombination in the QW. We observed a red shift of PL energy peak with the increase of Bi concentration due to band gap energy decrease as expected[5,35]. The PL spectra present a broad and asymmetric shape, with a low energy tail

typically attributed to localized excitons recombination, while the high energy band is related to free exciton recombination. At low temperature, PL is usually dominated by localized excitons occupying low energy states caused by Bi clusters, composition fluctuations and lattice disorder[28-30].

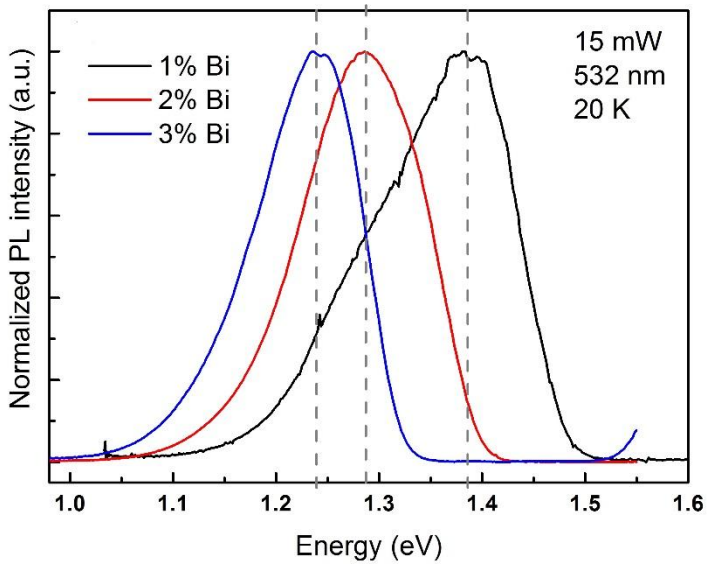

Figure 5: PL spectra of $GaAs_{(1-x)}Bi_x$/GaAs QW (10 nm) grown on (311)B GaAs substrate for nominal concentrations of 1%, 2% and 3% Bi, measured at low-temperature (20 K) and P_{EXC} = 15 mW.

The samples present an improvement of PL intensity and linewidth as the Bi concentration increases from 1% to 3%, which is not an expected result, since the large difference in atomic size between As and the substitutional Bi atom should introduce defects, and thus degrade the material quality with rising Bi composition. However, some previous studies on GaAsBi bulk (100) show that PL intensity first improves and then decreases as a threshold Bi percentage is reached[31,32]. In this way, our PL results could be interpreted as a consequence of competition mechanisms for generation and reduction of structural defects. As mentioned previously, our QW layers were grown at low temperatures. When the growth temperature is lower than the optimal GaAs growth temperature, native defects related to nonradiative energy states such as As antisites and Ga vacancies are usually generated in the material[11,14,15,32]. On the other hand, when a small amount of Bi ($x < 0.045$) is incorporated during GaAs growth at low temperatures, Bi atoms provide localized states close to the maximum of the valence band due to Bi-pairs and Bi-clusters formation[31]. These act as trapping centers for bound holes which can recombine radiatively. Simultaneously, Bi could act as a

surfactant which improves the material quality by reducing the defects due to low temperature growth[33]. Both features reduce the carrier loss by nonradiative centers and enhance the PL efficiency at rising Bi concentrations. After this condition, when the Bi amount is higher, the Bi-related defects start to become significant and might degrade the material quality[31].

The observed PL FWHM shrinkage with increasing values of Bi concentration (Fig.6 and 8(c)) is consistent with the enhancement of PL intensity due to a reduction of GaAs defects and increase of Bi localized states at this growth condition. The PL results are in agreement with FT-Raman data.

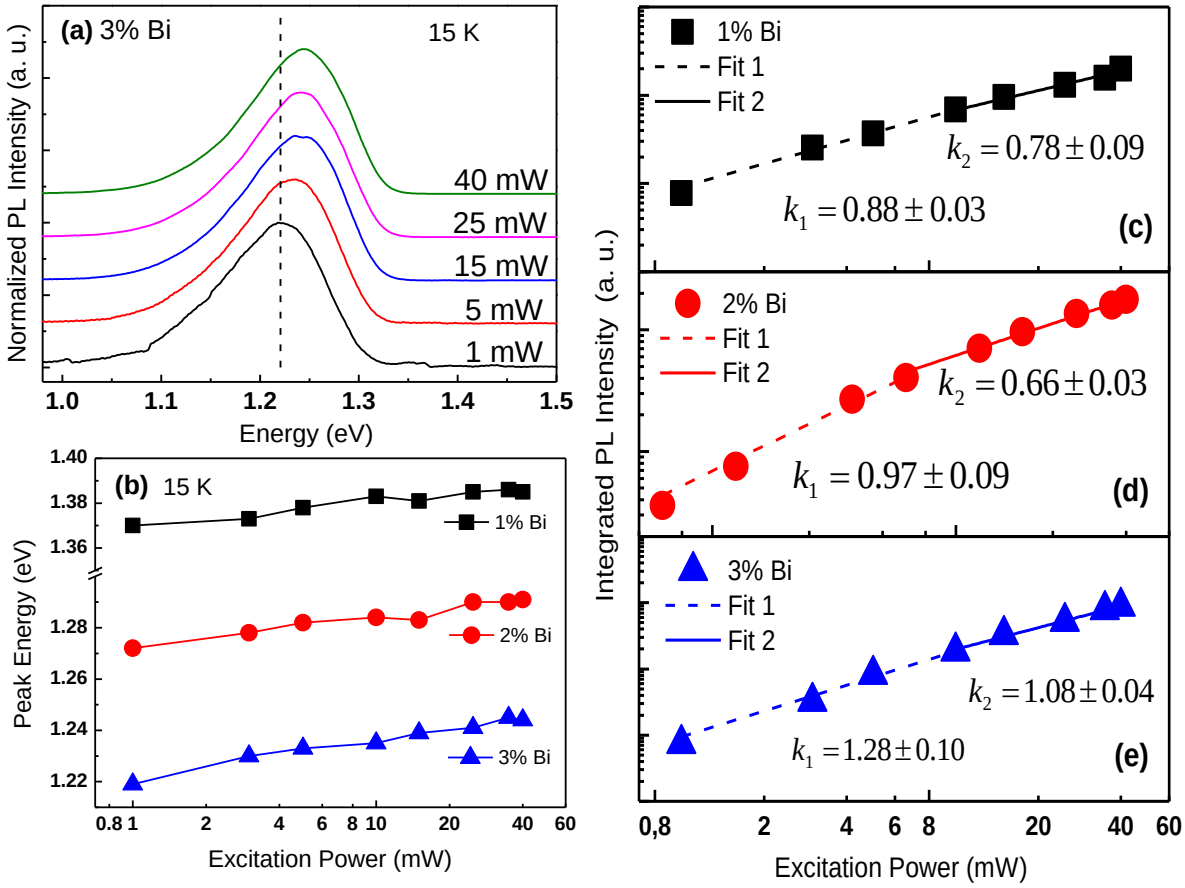

Figure 6: (a) Normalized PL spectra for the 3% Bi samples at 15 K for different P_{EXC} (b) PL peak energy as function of P_{EXC} for 1, 2 and 3% Bi. (c-e): Integrated PL intensity (I_{PL}) as function of P_{exc} for 1, 2 and 3% Bi at 15 K. The dashed lines illustrate the fitting using equation: $I_{PL} = \beta P_{exc}^{k}$.

Fig.6(a) shows the normalized PL spectra for $GaAs_{0.97}Bi_{0.03}$ QW sample at 15 K as a function of laser excitation power (P_{EXC}). As can be seen in Fig.6(a) the PL peak blue-shifts with the increase of P_{EXC}. This behavior is usually observed in highly perturbed systems such as

dilute nitride alloys and is associated with exciton localization effects. However, for $GaAs_{(1-x)}Bi_x$ it is well known that this effect is due to the occurrence of localized states near the top of the valence band. As explained previously, such localized states are expected to form in the regions with higher local Bi concentrations, which can be due to Bi-clusters and Bi-related defects.

The integrated PL intensity (I_{PL}) as function of P_{EXC} is shown in Fig.6(c-e) and its respective fitting curve using the power law $I_{PL} = \beta P_{EXC}^{k}$ [34], where I_{PL} is the integrated PL intensity, β and k are fitting parameters. We identified two different regimes for carrier radiative recombination as function of P_{EXC} and, consequently, two *k* values (k_1 and k_2) for each sample. At low P_{EXC} regime, the PL peak is at lower energy (Fig.6(b)) and the PL emission is governed by carriers occupying localized states which recombine radiatively, since these states are less energetic than native nonradiative defects and close to the valence band maximum. The obtained value of k_1 is < 1 for samples with 1% and 2% Bi which corresponds to the emission related to localized excitons. We also remarked that for the 3% Bi samples k_1 is roughly 1 which evidences important contribution of free excitons. However, at higher P_{EXC} regime we have obtained k_2 <1 for all samples, which could indicate a saturation effect due to the maximum carrier occupation of localized states. At this condition, the recombination process is dominated by free excitons which is limited by non-radiative recombination centers as the P_{EXC} is increased, reducing the PL efficiency as compared to low P_{EXC}. The non-radiative centers are usually more energetic than Bi related defects which are observed in bulk layers and $GaAs_{(1-x)}Bi_x$/GaAs QW. This effect is also evidenced by the observed blue shift of the PL peak as the P_{EXC} is increased as shown in Figure 6(b) [35-37]. Finally, since the *k values are* smaller for lower Bi concentrations, we conclude that the nonradiative losses of free excitons are smaller in the 3% Bi sample, which reflect an enhanced sample quality for higher Bi% content samples.

Fig.7(a) shows the temperature dependence of PL spectra for 3% Bi QW sample. As expected a red-shift of PL energy peak due to the decrease of the band gap energy with the increase of temperature was observed. However, the effects of exciton localization, due to alloy disorder and potential fluctuations, result in a temperature dependence of the PL peak position which cannot be explained by the standard Varshni's model[38]. This effect is probably due to the well-known ”S-shaped” behavior of disordered semiconductors including GaAsBi[29,32,37,39]. At higher temperatures and for higher P_{EXC} the PL spectra are expected to be dominated by free excitons[35-37]. As shown in Fig.7(b), the PL peak energy decreases with the temperature and the PL spectra gets broader. The S-shape behavior could not be evidenced here because the intensity of the PL signal is very small at higher temperatures. In general, our results are similar to previous reports on the PL of GaAsBi QWs grown on GaAs (100) substrates[29,40].

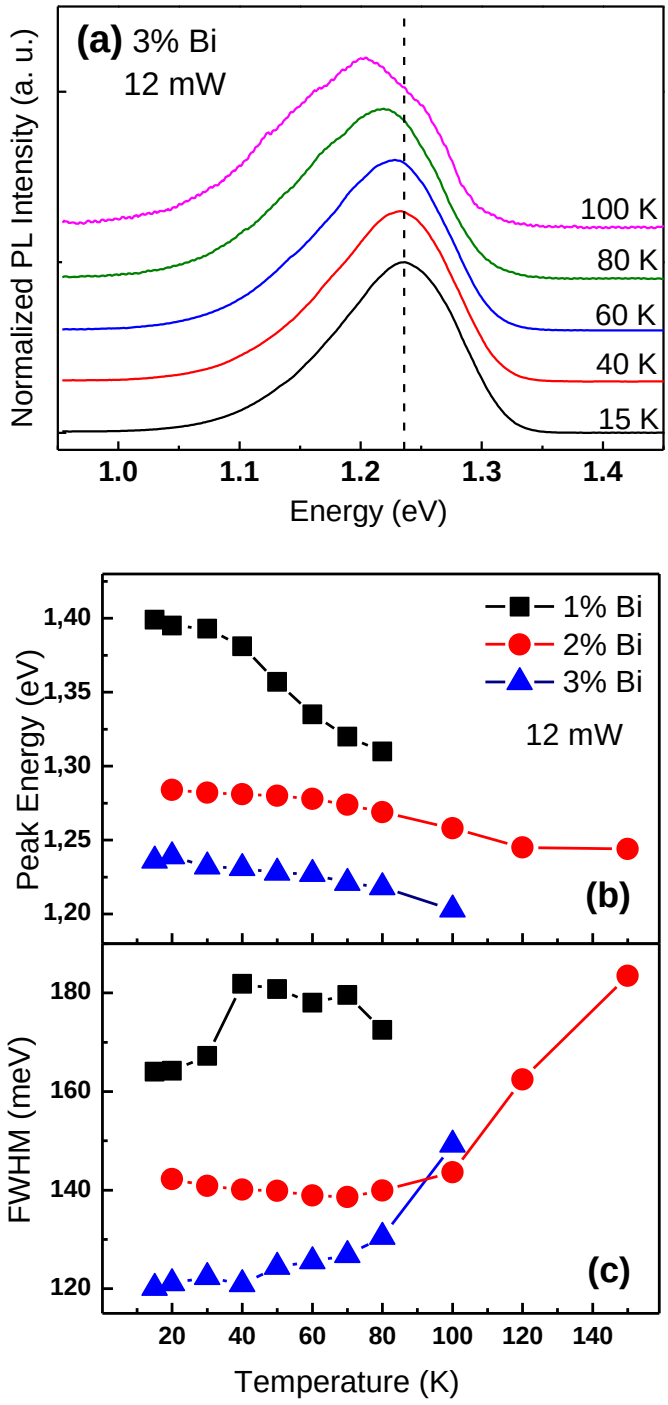

Figure 7: (a) Normalized PL spectra at 12 mW as function of temperature for samples with 3% Bi, (b) PL peak energy and (c) FWHM as function of temperature.

In order to investigate further the temperature dependence of PL intensities, we first fitted the data using a simple Arrhenius equation (not shown here). However, the fitting was not satisfactory as two distinct behaviors were observed indicating two activation energies. Therefore, we have included an additional energy term in the original equation:

$$I_{PL}(T)/I_0 = 1/[1 + C_1 exp(-E_1/k_B T) + C_2 exp(-E_2/k_B T)] \qquad (2)$$

where I_{PL} is the integrated PL intensity, A_1 and A_2 *are* constant related to the density of nonradiative centers, E_1 and E_2 are activation energies of these centers, k_B Boltzmann constant, T the temperature and I_0 the approximate PL intensity when $T \rightarrow 0$ [29,41,42]. A plot of $ln((I_0/I)-1)$ versus $1/k_BT$ is shown in Fig.8 and the activation energies obtained by these fittings. Even at very low Bi concentration, Bi atoms in GaAs host lattice tend to form localized pairs and clusters which have different configurations and binding energies[5,43], alloy disorder and potential fluctuation. They are usually associated with two groups with different activation energies: one ranges from 8 to 17 meV and is related to Bi clusters and Bi pair[5,29,41], and the other energy around 50 meV is related to alloy disorder[41,44-46]. At higher Bi concentrations, the localized energy levels still exist, but they are not effective for the PL recombination due to the fact that the maximum of the valence band moves up and the localized states merge in the valence band (VB). For the 1% Bi QW sample we obtained activation energies values of 13 ± 1 meV and 4.1 ± 0.4 meV which can be related to carriers at localized states due to different Bi clusters. On the other hand, for the 2% and 3% Bi QW samples distinct values of activation energies were obtained and which can be associated with both types of defects. Particularly, for the 2% Bi sample an activation energy of 53 meV was determined and attributed to alloy disorder caused by Bi incorporation fluctuation. Similar values for activation energies were reported for (100) GaAsBi QWs[29].

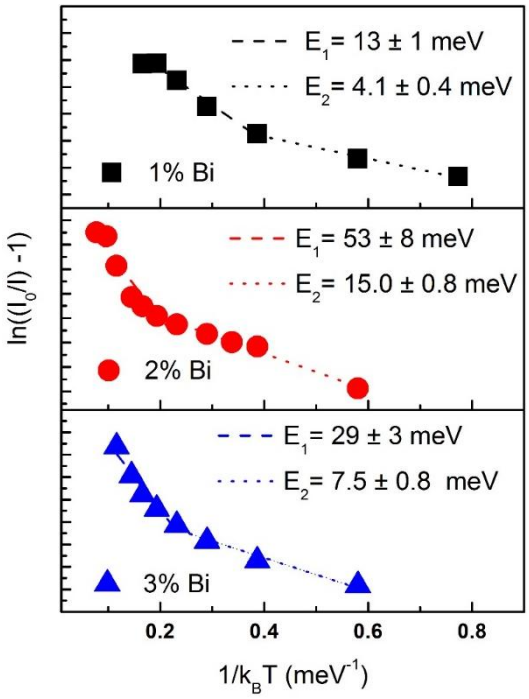

Figure 8: Arrhenius plot of PL intensity of QWs for Bi concentrations of 1, 2 and 3% Bi. The dashed lines illustrate the fitted lines using equation (2).

Conclusion

In conclusion, we have investigated the structural and optical properties of $GaAs_{1-x}Bi_x$/GaAs QWs grown on (311)B GaAs orientated substrates. Our results evidence important structural disorder and exciton localization. The Raman scattering results demonstrate that the relative intensity of TO and LO GaAs phonon modes changes with increasing Bi composition which indicates possible reduction of the structural disorder with increasing Bi incorporation. Moreover, PL spectra present a reduction of the linewidth and enhancement of PL intensity as Bi concentration increases. This behavior may be related to an important reduction of the density of nonradiative defects due to the Bi incorporation and increase of localized states. Finally, the determination of the activation energies from the temperature dependence of PL confirmed two distinct types of defects related to the Bi incorporation, namely Bi clusters and pairs, and alloy disorder and potential fluctuation.

Acknowledgements: We would like to acknowledge the financial supports from Fundação de Amparo a Pesquisa do Estado de São Paulo (FAPESP) grant numbers 12/24055-6, 14/50513-7 and 16/10668-7,CNPq, CAPES and the Scientific and Technological Research Council of Turkey (TUBITAK), project number 115F063.

References

[1] Sweeney S J and Jin S R 2013 *J. Appl. Phys.* **113** 043110

[2] Wang L, Zhang L, Yue L, Liang D, Chen X, Li Y, Lu P, Shao J and Wang S 2017 *Crystals* **7** 63

[3] Francoeur S, Seong M-J, Mascarenhas A, Tixier S, Adamcyk M and Tiedje T 2003 *Appl. Phys. Lett.* **82** 3874

[4] Alberi K, Wu J, Walukiewicz W, Yu K M, Dubon O D, Watkins S P, Wang C X, Liu X, Cho Y-J and Furdyna J 2007 *Phys. Rev. B*. **75** 045203

[5] Usman M, Broderick C A, Lindsay A and O'Reilly E P 2011 *Phys. Rev. B* **84**, 245202

[6] Marko I P, Broderick C A, Jin S, Ludewig P, Stolz W, Volz K, Rorison J M, O'Reilly E P and Sweeney S J 2016 *Sci. Rep.* **6,** 28863

[7] Beaudoin M, Lewis R B, Andrews J J, Bahrami-Yekta V, Masnadi-Shirazi M, O'Leary S K, Tiedje T 2015 *J. Cryst. Growth* **425,** 245–249

[8] Broderick C A *et al* 2014 *Phys. Rev. B* **90,** 195301

[9] Broderick C A, Usman M and O'Reilly E P 2013 *Phys. Status Solidi Basic Res.* **250,** 773–778

[10] Pettinari G, Polimeni A, Capizzi M, Blokland J H, Christianen P C M, Maan J C, Young E C and Tiedje T 2008 *Appl. Phys. Lett.* **92,** 262105

[11] Puustinen J, Wu M, Luna E, Schramm A, Laukkanen P, Laitinen M, Sajavaara T and Guina M 2013 *J. Appl. Phys.* **114,** 243504

[12] Lewis R B, Masnadi-Shirazi M and Tiedje T 2012 *Appl Phys Lett* **101** 082112

[13] Lu X, Beaton A D, Lewis R B, Tiedje T and Whitwick M B 2008 *Appl Phys Lett* **92** 192110

[14] Liu X, Prasad A, Nishio J and Weber E R 1995 *Appl Phys Lett* **67** 279

[15] Gebauer J, Börner F and Krause-Rehberg R 2000 *J Appl Phys* **87** 8368

[16] Luo G, Yang S, Jenness G R, Song Z, Kuech T F and Morgan D 2017 *NPG Asia Materials* **9** e345

[17] Mooney P M, Watkins K P, Jiang Z, Basile A F, Lewis R B, Bahrami-Yekta V, Masnadi-Shirazi M, Beaton D A and Tiedje T 2013 *J Appl Phys* **113** 133708

[18] Luna E, Wu M, Puustinen J, Guina M and Trampert A 2015 *J Appl Phys* **117** 185302

[19] Lemine O M, Alkaoud A, Avanco Galeti H V, Orsi Gordo V, Galvão Gobato Y, Bouzid H, Hajry A, Heninie M 2014 *Superlattice. Microst.* **65**, 48-55

[20] Henini M, Ibáñez J, Schmidbauer M, Shafi M, Novikov S V, Turyanska L, Molina S I, Sales D L, Chisholm M F and Misiewicz J 2007 *Appl. Phys. Lett.* **91** 251909

[21] Kudrawiec R *et al* 2009 *Microelectr. J.* **40,** 537–539

[22] Steele J A, Lewis R A, Henini M, Lemine O. M. and Alkaoud A Raman 2013 *J. Appl. Phys.* **114,** 193516

[23] Balanta M A G *et al* 2016 *J. Phys. D. Appl. Phys.* **49,** 355104

[24] Lewis R B, Masnadi-Shirazi M and Tiedje T 2012 *Appl. Phys. Lett.* **101,** 082112.

[25] Fitouri H, Moussa I, Rebey A, Fouzri A, El Jani B 2006 *J. Cryst. Growth* **295,** 114-118

[26] Moussa I, Fitouri H, Rebey A, El Jani B 2008 *Thin Solid Films* **516,** 8372-8376

[27] Steele J, Structural and optical studies of GaAs1-xBix and p-Bi203 for optoelectronic devices, Doctor of Philosophy thesis, School of Physics, University of Wollongong, 2015.

[28] Francoeur S, Tixier S, Young E, Tiedje T and Mascarenhas A 2008, *Phys. Rev. B* **77**, 085209

[29] Donmez O, Erol A, Arikan M C, Makhloufi H, Arnoult A and Fontaine C 2015 *Semicond. Sci. Technol.* **30,** 94016

[30] Kopaczek J, Linhart W M, Baranowski M, Richards R D, Bastiman F, David J P R and Kudrawiec R 2015 *Semicond. Sci. Technol.* **30,** 94005

[31] Lu X, Beaton D A, Lewis R B, Tiedje T and Zhang Y 2009 *Appl. Phys. Lett.* **95,** 41903

[32] Mohmad A R, Bastiman F, Hunter C J, Richards R D, Sweeney S J, Ng J S, David J P R and Majlis B Y 2014 *Phys. Status Solidi Basic Res.* **251,** 1276–1281

[33] Tixier S, Adamcyk M, Young EC, Schmid JH, Tiedje T 2003 *J Crytal Growth* **251** 449

[34] Schmidt T, Lischka K and Zulehner W 1992 *Phys. Rev. B* **45**, *8989*

[35] Shakfa M K, Kalincev D, Lu X, Johnson S R, Beaton D A, Tiedje T, Chernikov A, Chatterjee S and Koch M 2013 *J. Appl. Phys.* **114**, 164306

[36] Kudrawiec R *et al* 2009 *J. Appl. Phys.* **106,** 023518

[37] Mazzucato S, Lehec H, Carrère H, Makhloufi H, Arnoult A, Fontaine C, Amand T and Marie X 2014 *Nanoscale Res. Lett.* **9,** 19

[38] Varshni Y P 1967 *Physica* **34,** 149–154

[39] Wilson T, Hylton N P, Harada Y, Pearce P, Alonso-Álvarez D, Mellor A, Richards R D, David J P R and Ekins-Daukes N J 2018 *Scientific Reports* **8** 6457

[40] Mazur Y I, Dorogan V G, Schmidbauer M, Tarasov G G, Johnson S R, Lu X, Ware M E, Yu S Q, Tiedje T, Salamo G J 2013 *J Appl Phys* **113** 144308

[41] Mazzucato S, Boonpeng P, Carrère H, Lagarde D, Arnoult A, Lacoste G, Zhang T, Balocchi A, Amand T, Marie X 2013 *Semicond. Sci. Technol.* **28,** 22001

[42] Lu, T. *et al.* 2014 *Sci. Rep.* **4,** 6131

[43] Zhang Y, Mascarenhas A and Wang L W 2005 *Phys. Rev. B* **71**,155201

[44] Imhof S *et al* 2010 *Appl. Phys. Lett.* **96** 131115

[45] Imhof S *et al* 2011 *Appl. Phys. Lett.* **98** 161104

[46] Yoshimoto M, Itoh M, Tominaga Y and Oe K 2013 *J. Cryst. Growth* **378**, 73-76